iScience

Article

Altered m6A RNA methylation profiles in depression implicate the dysregulation of discrete cellular functions in males and females

Graphical abstract

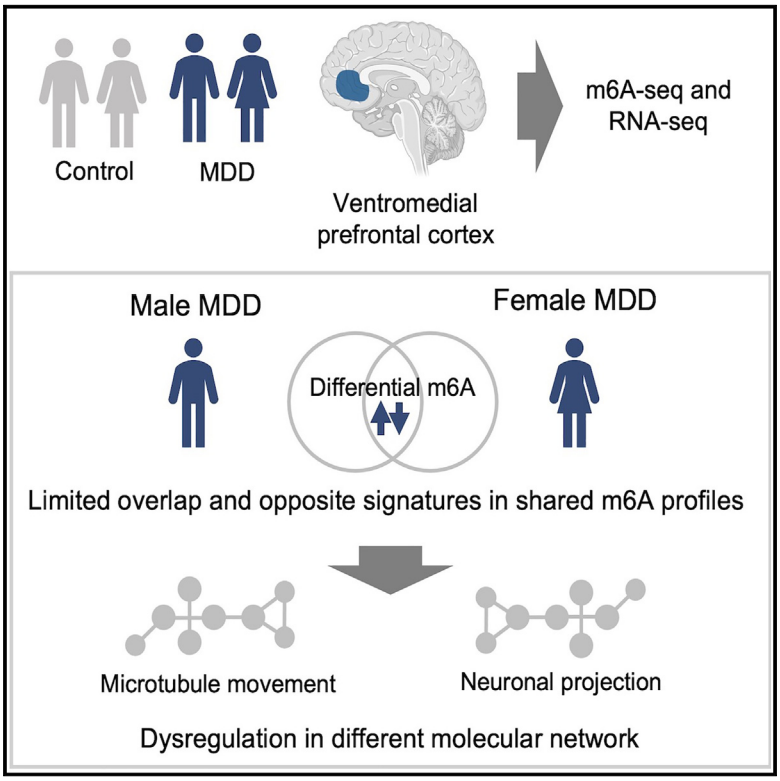

Highlights

- Distinct m6A profiles were observed in the human ventromedial prefrontal cortex of MDD
- Differentially regulated m6A in males and females with depression showed opposite trends
- m6A may lead to dysregulation in different molecular networks in males and females with MDD

Authors

Haruka Mitsuhashi, Rixing Lin, Anjali Chawla, Naguib Mechawar, Corina Nagy, Gustavo Turecki

Correspondence

gustavo.turecki@mcgill.ca

In brief

Health sciences; Medicine; Medical specialty; Psychiatry; Natural sciences; Biological sciences; Omics.

Mitsuhashi et al., 2024, iScience *27*, 111316
December 20, 2024
https://doi.org/10.1016/j.isci.2024.111316

CellPress

iScience

CellPress
OPEN ACCESS

Article

Altered m6A RNA methylation profiles in depression implicate the dysregulation of discrete cellular functions in males and females

Haruka Mitsuhashi,[1,2] Rixing Lin,[3] Anjali Chawla,[1,2] Naguib Mechawar,[1,2,4] Corina Nagy,[1,2,4,5] and Gustavo Turecki[1,2,4,5,6,*]
[1]McGill Group for Suicide Studies, Douglas Mental Health University Institute, McGill University, Montreal, QC H4H 1R3, Canada
[2]Integrated Program in Neuroscience, McGill University, Montreal, QC H3A 0G4, Canada
[3]Princeton Neuroscience Institute, Princeton University, Princeton, NJ 08544 USA, USA
[4]Department of Psychiatry, McGill University, Montreal, QC H3A 0G4, Canada
[5]These authors contributed equally
[6]Lead contact
*Correspondence: gustavo.turecki@mcgill.ca
https://doi.org/10.1016/j.isci.2024.111316

SUMMARY

Adverse environmental stress represents a significant risk factor for major depressive disorder (MDD), often resulting in disrupted synaptic connectivity which is known to be partly regulated by epigenetic mechanisms. N^6-methyladenosine (m6A), an epitranscriptomic modification, has emerged as a crucial regulator of activity-dependent gene regulation. In this study, we characterized m6A profiles in the ventromedial prefrontal cortex (vmPFC) of individuals with MDD. Using m6A sequencing, we identified a total of 30,279 high-confidence m6A peaks, exhibiting significant enrichment in genes related to neuronal and synaptic function. The m6A peaks between males and females with MDD that passed the significance threshold showed opposite m6A patterns, while the threshold-free m6A patterns were concordant. Distinct m6A profiles were found in MDD for each sex, with dysregulation associated with microtubule movement in males and neuronal projection in females. Our results suggest the potential roles of m6A as part of the dysregulated molecular network in MDD.

INTRODUCTION

There are 170 known RNA modifications, among these, m6A methylation (m6A) is the most abundant RNA modification in messenger RNA (mRNA) in mammals, with a frequency of 0.1%–0.6% of all adenosines.[1,2] m6a is typically located in a consensus motif (DRACH) and enriched in near 3′UTR and stop codon. m6A is reversible; it is catalyzed by a writer complex consisting of methyltransferase-like 3 (METT3), methyltransferase-like 4 (METT14), and WT1 associated protein provided (WTAP) and removed by alkB homolog 5 (ALKBH5) and the fat mass and obesity-associated protein (FTO).[3–5] m6A is recognized by different types of reader proteins and depending on the given reader, m6A either influences stability, translation efficiency, degradation, splicing, or nuclear export of the target transcripts.[6] Although the mechanism of how reader proteins target specific m6A transcripts is still unknown, we know dynamic post-transcriptional gene regulation by m6A is essential, especially in the central nervous system.[7,8]

Given the brain's relatively high abundance of m6A, this modification has emerged as a crucial regulator of both rapid and long-term changes in gene expression.[9] Transcripts associated with synaptic and neuronal functions display significant levels of m6A, with these patterns subject to alterations in response to neuronal activity. Research to date has focused on learning and memory and revealed that loss of m6A function by the depletion of m6A machinery leads to behavioral deficits and disruptions in neuronal circuits.[10–12] Notably, m6A methylated transcripts are enriched at synapses, suggesting a role in regulating brain plasticity in response to environmental cues.[13,14] In support of this, studies in mice have demonstrated that alterations in m6A levels in the brain following acute stress coincide with changes in m6A-marked transcripts associated with stress response and neuroplasticity.[15] These investigations highlight m6A's significance as a key player in the stress response and its potential role in psychiatric disorders.

Major depressive disorder (MDD) is a complex disorder that affects approximately 300 million individuals globally.[16] Its development involves a complex interplay of genetic predisposition and environmental influences, and epigenetic mechanisms, at least in part, mediate its interaction. Chronic stress is a well-known risk factor for MDD and the neuronal adaptations in response to stress are critical processes related to its onset.[17] Dysregulation of the hypothalamic pituitary adrenal (HPA) axis, the monoamine system, and inflammation, among others, have been associated with the etiopathogenesis of depression.[18] Another common finding in MDD is neuronal

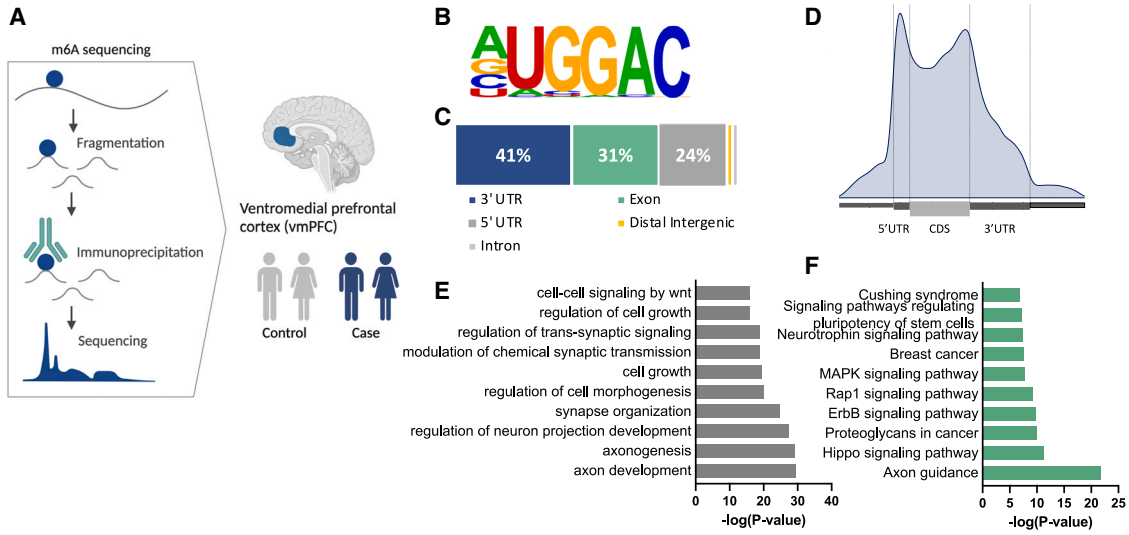

Figure 1. Characteristic of m6A peaks in the human brain

(A) Schematic overview of the m6A-seq and samples used in this study. Optimized m6A-seq protocol was used to profile m6A on the vmPFC of the matched males and females with MDD and psychiatrically healthy controls (N = 9–10/group; total *N* = 39).

(B) Sequence motif of the m6A-containing peak regions shows GGAC enrichment (*p*-value: 1e-302).

(C) The percentage of m6A peaks located across the gene body.

(D) The distribution of m6A peaks on mRNA transcripts.

(E) Top 10 biological GO terms of m6A peaks showed enrichment in genes associated with neuronal and synaptic function.

(F) Top 10 KEGG terms of m6A peaks showed enrichment in signaling pathways similar to the previous m6A study in the human brain.

atrophy and synaptic loss, resulting in reduced volume of specific brain regions crucial for mood regulation and stress response. Interestingly, there is some evidence that these morphological changes can be reversed with antidepressant treatment.[19] Neuronal guidance cues such as netrin, slit, semaphorins, and ephrins finely regulate structural changes in the brain. These cues guide the growth of axons and dendrites toward their targets and regulate synaptic plasticity.[20] Interestingly, a recent study indicates that m6A contributes to axon guidance. Specifically, the m6A reader protein YTHDF1 has been found to promote the translation of Robo 3.1, a receptor crucial for slit protein signaling in axon guidance from the Roundabout (Robo) family.[21]

Considering the established roles of m6A in stress response and neuroplasticity systems that together can contribute to neuroanatomical changes observed in MDD, investigating m6A holds promise for unraveling the molecular mechanism underlying MDD. Furthermore, m6A serves as a responsive marker of stress. Therefore, we conducted comprehensive postmortem profiling of m6A status in human postmortem vmPFC of both males and females diagnosed with MDD and matched controls to identify m6A patterns underlying the sex-influenced mechanism of MDD. Threshold-free m6A patterns between males and females with MDD showed concordant trends; however, differential m6A peaks showed opposite signatures with enrichment in genes linked to histone modification. Further analysis showed the sex-specific differential m6A patterns associated with MDD, involving cellular microtubule movement in males and neuronal projections in females.

RESULTS

N^6-methyladenosine methylation landscape in the human brain

To investigate the role of m6A in the human brain, we focused on the vmPFC, a region that has been implicated in the pathophysiology of MDD.[22] We examined human postmortem brain samples from both male and female donors, half who died during an episode of MDD, and the other half, matched neurotypical controls (Figure 1A; Table S1). To profile the m6A landscape, we used an antibody based methylated RNA immunoprecipitation followed by sequencing (m6A-seq), which we optimized for use in postmortem brain tissue. Using stringent peak-calling filters, we identified a total of 30,279 high-confidence m6A consensus peaks (FDR< 0.05, fold change >1.5) (Figures S1A and S1B). The peaks were distributed among 12,691 transcripts, with an average of 2.4 m6A peaks per gene. Motif enrichment analysis of m6A peaks demonstrated a robust enrichment of the GGAC consensus motif (*p*-value: 1e-302), affirming the high quality of our peak set (Figure 1B). The distribution of m6A peaks showed a particular enrichment in the junction of the 3′ untranslated region (3′UTR) and the coding sequence (CDS) and 5′ untranslated region (5′UTR), consistent with previous findings (Figures 1C and 1D).[23] Gene ontology (GO) analysis of m6A-modified transcripts revealed a significant enrichment (*p*-value <0.05) of genes related to axon development, neuron projection development, and synapse organization (Figure 1E). Furthermore, KEGG pathway analysis revealed that m6A modifications were associated with the Hippo signaling pathway, ErbB signaling pathway, and MAPK signaling pathway, all closely

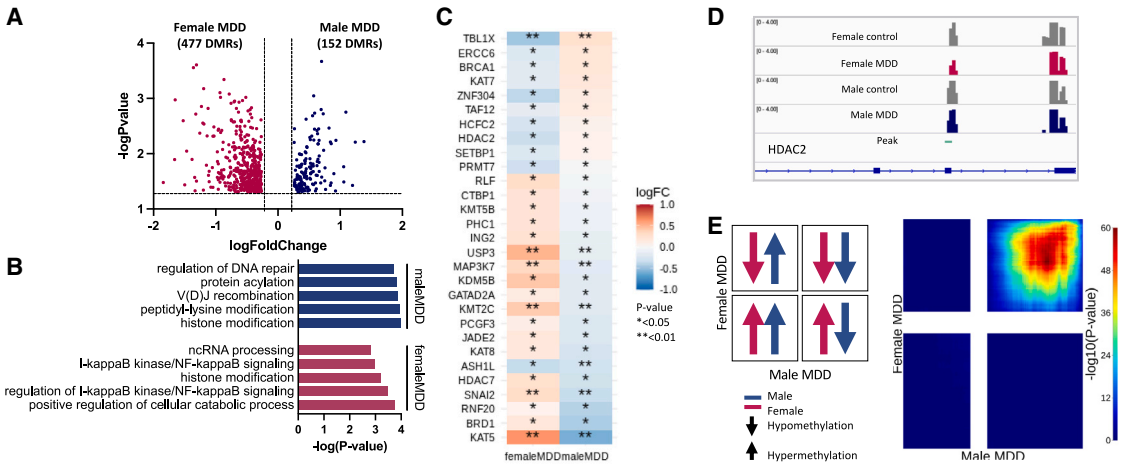

Figure 2. m6A peak profile of male and female with MDD shows the opposite signature

(A) Volcano plot showing DMR identified between males and females with MDD. 153 DMRs were unique to male MDD (blue) and 477 DMRs were unique to female MDD (pink).

(B) Top 5 biological Gene ontology (GO) terms related to m6A peaks associated with male MDD and female MDD, demonstrating enrichment in genes linked to histone modification.

(C) Heatmap showing the methylation patterns of genes associated with histone modifications. The color shows log fold change of methylation levels in MDD compared to controls in each sex.

(D) IGV plot of the differentially methylated region (DMR) in HDAC2 located at chr6 113993352–113993500, showing an example of an opposite differential methylation pattern male and female with MDD.

(E) Threshold-free differential methylation patterns in males and females with MDD with rank-rank hypergeometric overlap (RRHO). The color of each heatmap is based on –log10 (*p*-value) from the hypergeometric test. The map in the right corner shows the shared hypomethylation between male MDD and female MDD.

linked to the development of the nervous system and neuronal differentiation in the brain (Figure 1F). These findings are consistent with previous research conducted on the human dorsal prefrontal cortex (dlPFC) and the mouse brain.[24,25]

N^6-methyladenosine methylation signatures in males and females with major depressive disorder

Emerging studies suggest males and females have distinct molecular profiles, particularly in the vmPFC.[26] Considering the sex influences in MDD prevalence and pathology, and possibly, in underlying biological processes,[26,27] we accessed differences in m6A profiles using sex-disease interaction analyses. We detected a total of 629 differentially methylated regions (DMRs), including 152 peaks unique to male MDD and 477 peaks unique to female MDD (*p*-value <0.05, fold change >1.2; Figure 2A; Table S2). GO analysis of the differentially methylated peaks revealed strong enrichment in genes associated with histone modifications in MDD regardless of sex (Figure 2B). However, many of these histone-related genes were methylated in opposite directions between males and females with MDD. For instance, hypomethylated regions in females were hypermethylated in males or we observed the inverse (Figures 2C and 2D). These changes were not limited to genes related to histone modifications but several differentially m6A tagged genes showed an effect of moderation by sex, and some of those that were significant (*p*-value <0.05, fold change >1.2) were modified in the opposite direction. To see if this pattern holds in general, we used a threshold-free comparison, and a rank-rank hypergeometric overlap (RRHO) analysis and found an overall concordance in the direction of the methylation differences for males and females compared to controls (Figure 2E). This finding is consistent with our recent publications reporting overall similarity in cortical transcriptional signatures between males and females with MDD.[28,29]

Dysregulated N^6-methyladenosine methylation and gene expression patterns in microtubule movement in male major depressive disorder

Given that significant differentially methylated m6A peaks showed opposite patterns between males and females with MDD, we opted to explore within sex patterns of methylation by disaggregating the data. In males, the differential methylation result showed distinct m6A patterns between cases and controls, as shown in the heatmap (Figure S2A). We detected a total of 239 differentially methylated regions, including 98 hypomethylated peaks and 141 hypermethylated peaks (*p*-value <0.05, fold change >1.2; Figure 3A; Table S3). No significant difference was found in the number of DMR located at 3′UTR, CDS, or 5′UTR were similar (Figure S2B). GO analysis of hypermethylated peaks revealed enrichment in genes associated with histone acetylation and epithelial cilium movement whereas hypomethylated peaks showed enrichment in genes related to DNA-templated transcription elongation and protein signal transduction (Figure 3B).

Given that m6A is known to regulate the degradation or translation of the target transcript, we accessed the putative function of genes targeted by m6A. First, we examined changes in gene expression between cases and controls. A total of 1,285 genes were differentially expressed, including 691 down regulated genes and 594 upregulated genes (*p*-value <0.05, fold change

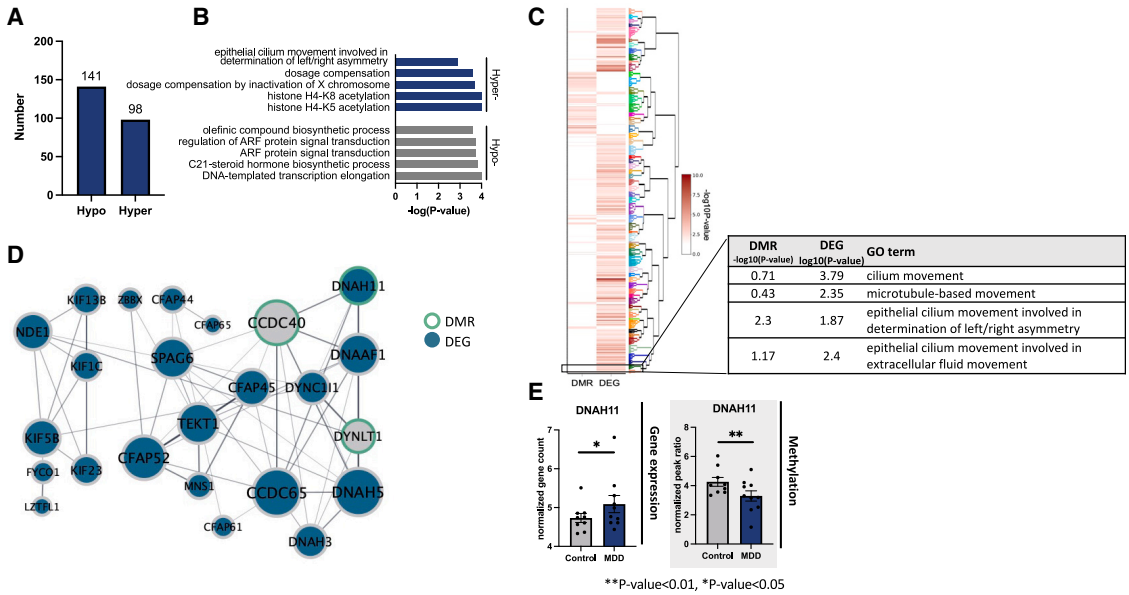

DMR -log10(P-value)	DEG log10(P-value)	GO term
0.71	3.79	cilium movement
0.43	2.35	microtubule-based movement
2.3	1.87	epithelial cilium movement involved in determination of left/right asymmetry
1.17	2.4	epithelial cilium movement involved in extracellular fluid movement

Figure 3. Differentially methylated regions in male MDD are associated with cilium movement

(A) The number of hypomethylated and hypermethylated DMR identified between male MDD and male control.

(B) The top 5 biological process GO enrichment terms of the hypermethylated peaks and hypomethylated peaks.

(C) Clustering heatmap of GO terms identified in DMRs and DEGs.

(D) Protein-protein network of genes annotated to microtubule-based movement cluster. Node size corresponds to the degree of interaction, node color indicates differential expression status, and node border color indicates differential methylation status. Edge width reflects the protein-protein interaction score. Protein with no interaction was removed.

(E) Bar plot showing methylation (right) and gene expression (left) levels of DNAH11. Data are represented as mean ± SEM.

>1.2; Figure S3A). GO analysis of differentially expressed genes (DEG) indicated that downregulated genes were enriched for functions related to synaptic regulation, while upregulated genes were enriched for functions related to axonal regulation and neuronal projection (Figure S3B). Dysregulation of genes related to neuronal and synaptic function in male MDD aligns with the previous findings on sex differences in MDD. However, upon comparing the results of DMRs and DEGs, we observed a limited overlap, with only 11 genes identified as being both DMRs and DEGs. These findings align with prior studies that reported minimal overlap between DMRs and DEGs in the field of m6A studies.[25,30] Additionally, we investigated the correlation between the DMRs and the corresponding gene expression levels. No significant correlation between hypermethylation and corresponding genes (R^2 = 0.04, p-value = 0.042), as well as hypomethylation and the expression of corresponding genes (R^2 = 0.08, p-value = 0.014) were found (Figure S3C).

In addition to directly affecting gene expression levels, m6A can regulate translation through reader proteins without significantly altering overall gene expression. Given the wide range of impacts that m6A can have on target transcripts, we next investigated the biological network dysregulated in MDD by examining overlaps in biological processes regulated by DMRs and DEGs. To accomplish this, we conducted GO clustering using the union of significant GO terms identified in both analyses (p-value <0.05; Figure 3C). Using this approach, a total of 61 GO clusters were identified. Among these, the GO term in cluster #61 showed shared enrichment in DMR and DEG (Table S4). The genes in cluster #61 were enriched for functions related to microtubule-based movement. To unravel the interconnectivity within this cluster, we performed Protein-Protein Interaction (PPI) network analysis using DMR-genes and DEG annotated to the cluster #61 (Figure 3D). Hub genes, such as Dynein Axonemal Heavy Chain 5 (DNAH5) and Coiled-Coil Domain Containing 65 (CCDC65), were found to interact with DMR genes. Within the network, DNAH11 was both a DMR and DEG. Its gene expression levels were elevated in MDD, while the methylation levels were decreased (Figure 3E). This suggests a potential regulatory role through m6A modification, hinting at involvement in processes such as degradation or translation.

Dysregulated N^6-methyladenosine methylation and gene expression patterns in neuronal projection in female major depressive disorder

Next, we investigated the differences in m6A profiles between female cases and controls. The heatmap of methylation scores illustrated distinct m6A profiles between groups (Figure S2C). In total, we identified 696 DMRs, comprising 241 hypomethylated and 455 hypermethylated peaks (p-value <0.05, fold change >1.2; Figure 4A; Table S5). The number of female DMRs was approximately three times the number identified in males. Like males, the DMRs were nearly equally distributed along mRNA transcripts (Figure S2D). GO analysis revealed that hypermethylated peaks were enriched in genes associated with the regulation of neurogenesis and the regulation of dendrite morphogenesis (Figure 4B). In contrast, hypomethylated peaks

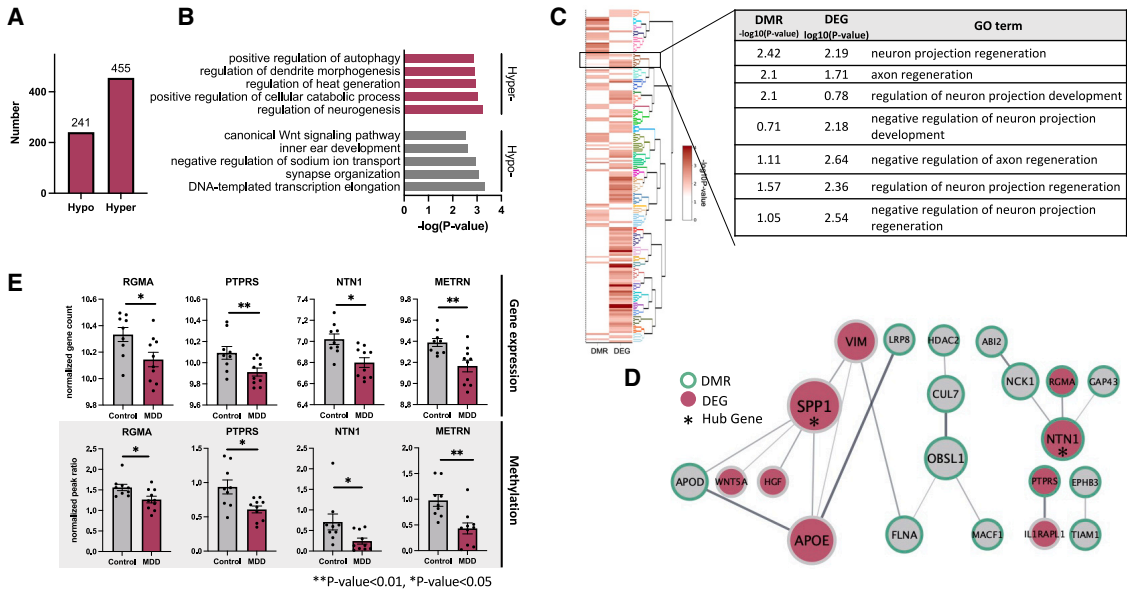

Figure 4. Differentially methylated regions in female MDD are associated with neuronal projection development

(A) The number of hypomethylated and hypermethylated DMR identified between female MDD and male control.

(B) The top 5 biological process GO enrichment terms of the hypermethylated peaks and hypomethylated peaks.

(C) Clustering heatmap of GO terms identified in DMRs and DEGs.

(D) Protein-protein network illustrating genes annotated to the neuronal projection development cluster. Node size corresponds to the degree of interaction, node color denotes differential expression status, and node edge color signifies differential methylation. Edge width reflects the protein-protein interaction score.

(E) Bar plots showing the methylation and gene expression levels of genes that exhibited differential methylation (down) and expression (up) within the neuronal projection development cluster. Data are represented as mean ± SEM.

were enriched in genes related to DNA template transcription regulation and synapse organization.

Examining differential expression, we identified a total of 566 altered genes, including 308 down regulated and 258 upregulated genes (p-value <0.05, fold change >1.2; Figure S3D). GO analysis of DEGs indicated that downregulated genes were enriched for functions related to the immune system such as macrophage activation and the regulation of cytokine production, while upregulated genes were enriched for functions related to extracellular structure and matrix organization (Figure S3E). Similar to the findings observed in males, overlaps between DMRs and DEGs were observed only for 13 genes. In addition, no significant correlations were found between the fold-change of DMRs and the expression levels of corresponding genes in either hypermethylated DMRs (R^2 < 0.01, p-value = 0.223) or hypomethylated DMRs (R^2 < 0.01, p-value = 0.969; Figure S3F).

Next, as for males, we performed GO clustering using only the significant terms identified for DMRs and DEGs (Figure 4C). Among the 34 clusters identified, cluster #6 is one of the clusters that exhibited enrichment in both DEG and DMR datasets (Table S6). Cluster #6 identified an enrichment in genes associated with neuron projection development. PPI network analysis of DMR genes and DEG within cluster #6 revealed several distinct networks. Secreted Phosphoprotein 1 (SPPI) emerged as a hub gene in the largest network, showcasing both direct and indirect interactions with DEG and DMR genes (Figure 4D). Notably, Netrin 1 (NTN1), a gene with significantly decreased expression (p-value = 0.022, logFoldChange = −0.40) and methylation levels (p-value = 0.019, logFoldChange = 0.32) in cases, was identified as a hub gene in another network subgroup (Figure 4E). NTN1 is recognized for its crucial role in axonal guidance and has previously been implicated in MDD.[31] Furthermore, NTN1 exhibited interactions with other DMR-genes, including Repulsive Guidance Molecule (RGMA), where both gene expression (p-value = 0.040, logFoldChange = −0.29) and methylation levels (p-value = 0.037, logFoldChange = 0.30) were significantly reduced in MDD (Figure 4E). Consistent with the observation for NTN1, RGMA plays a crucial role in axon guidance and neuronal survival, Matsunaga et al.[32]

Gene expression of N^6-methyladenosine methylation regulators in male and female major depressive disorder

Previous studies have demonstrated changes in the gene expression of m6A regulators in the context of MDD in brain regions specific manner.[33,34] Given that our DMR results showed a higher number of hypomethylated peaks compared to hypermethylated peaks in male MDD and a higher number of hypermethylated peaks in female MDD, we hypothesized that these changes might be reflected in the gene expression of m6A writers and erasers. Using our DEG results, we investigated whether the m6A writers, erasers, and readers were differentially expressed between controls and MDD in each sex. However, our results indicated no significant differences in the expression of any of the m6A regulators tested in both males and females with MDD (Figures S4A and S4B).

DISCUSSION

m6A profiles in the vmPFC of patients diagnosed with MDD revealed distinct m6A patterns between males and females. There were substantial methylation changes in MDD across sexes, and interconnectivity between DMR-genes and DEG showed m6A as a part of disrupted network, which was previously implicated in MDD.

Recent evidence from human brain studies suggests sex-influenced transcriptional changes in MDD.[26–28] Our findings are consistent with these transcriptional studies in that epitranscriptomic changes, which are shown to influence gene expression, showed unique patterns between males and females with MDD. Although genes associated with histone modification were enriched in both male and female MDD, their methylation patterns were in the opposite direction. Interestingly, the sex steroid hormone estrogen is recognized as a pioneering factor, initiating changes in chromatin structure, activating enhancer elements, and recruiting transcriptional machinery.[35,36] These actions lead to alterations in epigenetic modifications, enabling estrogen to regulate a wide range of target genes involved in diverse biological processes, such as cell proliferation, differentiation, and homeostasis. While there is limited literature on the interplay between sex steroid hormones and m6A machinery in the brain, RNA-binding motif protein 15 (RBM15), a component of the writer complex, has been identified as an estrogen-responsive gene in breast cancer cells.[37] Furthermore, the deletion of the m6A writer METTL3 in the female reproductive tract leads to changes in the stability of estrogen-responsive and progesterone-responsive genes in the uterus.[38] Although its role in the brain is unclear, the interaction between m6A and sex hormones suggests its potential role in menopause, which has been associated with MDD in females. The alterations in epitranscriptomic and epigenetic signatures triggered by estrogen could potentially underlie a broad spectrum of sex-associated differences observed in MDD.

Within the list of histone modification related genes, we identified histone acetyltransferases (HATs), and histone methyltransferases (HMTs). The interplay of m6A and histone modification could explain the altered histone modification patterns leading to sex-influenced molecular mechanisms in MDD.[39] m6A has been shown to participate in the degradation of histone modifiers, resulting in reduced levels of HATs or HMTs.[39] Furthermore, the depletion of Mettl3, an m6A writer, results in the loss of m6A and an increase in the expression of histone modifiers, contributing to abnormal gene expression associated with phenotypic abnormalities.[40] HDAC7 is one of the histone modifiers that shows sex-specific expression alteration following acute restraint stress in the hippocampus.[41] While there is limited literature on sex-specific altered expression of histone modification, widespread dysregulation of histone modification in MDD has been shown in clinical studies, human postmortem studies, and animal models of depression. For instance, HDAC2, one of the best studied HDACs, exhibited hypomethylation in female MDD and hypermethylation in male MDD.[42]

Previous studies have demonstrated the widespread dysregulation of cilia-related genes in psychiatric disorders, including MDD.[43] Our findings in males align with this observation, as we identified altered methylation and expression patterns of dynein genes (DNAH11, DNAH5, DYNLT1) and axoneme genes (CCDC40, CCDC65), which support microtubule-based cytoskeletal structure. Most brain cells, including neurons and astrocytes, possess primary cilia housing unique proteins such as dynein, axoneme, and kinesin.[44] These proteins enable primary cilia to detect extracellular cues and regulate signal transduction pathways, including Shh and Wnt signaling. Moreover, primary cilia in the brain are enriched with G-protein coupled receptors (GPCRs), including somatostatin receptor type 3, serotonin receptor 6 (5HT-6), and a subset of dopamine receptors (DR1, DR2, and DR5).[44,45] It has been suggested that primary cilia may play a role in activating these signaling pathways, which have implications for MDD and antidepressant treatments.[46,47]

Recent transcriptional studies observed increased neuroplasticity and neuronal connectivity and decreased microglia activation particularly in female MDD.[48,49] Our findings are in line with this, we observed decreased expression of genes associated with immune-related responses in female MDD, such as macrophage activation and cytokine activation. While a gene set directly related to immune response did not emerge among the shared GO terms between DMRs and DEGs, we did find a common enrichment of genes associated with neuronal connectivity and plasticity.

Netrin family proteins NTN1 and RGMA were both identified as DMR and DEG. NTN1 and RGMA share a ligand receptor called Neogenin-1 (*NEO*1), which is a transcriptional target of the sonic hedgehog (Shh) pathway. Shh pathway play a role in adaptive circuits by regulating axonal outgrowth and synaptic plasticity. In addition, RGMA stimulation in the adult neural stem suppressed the neurite outgrowth of newborn neurons, suggesting its function in regulating adult brain plasticity.[50] NTN1 has several other receptors, and it is binding to DCC has been associated with MDD.[31] NTN1/DCC signaling influences axonal guidance, dendritic growth, and synapse formation during development when the brain is susceptible to stress and key period for shaping neuronal circuits. In the adult brain, NTN1/DCC signaling guides synaptic connectivity, and dysregulated expression of DCC determines susceptibility to stress.[51,52] Chronic stress can modulate NTN1/DCC signaling activity through changes in epigenetic modification including miRNA.[53] Although the majority of these studies were conducted on males, our result implicates the possible dysregulation of NTN1/DCC signaling in females. NCK1, which has connectivity with NTN1, has been shown to have sex-specific deficits in hippocampal memory formation through changes in postsynaptic densities and synaptic densities.[54] Together, these data support the idea that m6A may contribute to the dysregulation of neuronal connectivity in female MDD. Although further investigations are needed, our study supports the landscape of RNA modifications in MDD showing clear sex differences in basic transcriptomic regulation. This work opens the door to identifying novel precision-based therapeutics.

Limitations of the study

Using m6A-seq we conducted a comprehensive and unbiased profile of m6A signatures in human postmortem vmPFC; however, we recognize that our study is not without limitations. Similar

to the majority of studies on m6A, our antibody-based m6A identification approach lacks single-nucleotide resolution. While existing methods relying on enzymatic conversion or direct RNA sequencing offer a potential solution to these limitations, applying such technologies to human postmortem tissues remains challenging.[55–57] Indeed, dissecting the cell-type-specific contributions in MDD is particularly important, given that different cell types have been implicated in MDD.[28,58]

The limited overlap between DMRs and DEGs and no significant correlation between fold change of DMRs and DEGs are not surprising given previous observations and suggest that changes in gene expression levels may not be temporally associated with m6A changes or that the impact of m6A on gene expression is not direct.[25,30,40] Although m6A has been shown to regulate gene expression by affecting the stability of target transcripts, the lack of overlap between DMRs and DEGs has been reported.[25,30] Previous studies have shown that m6A can impact protein levels without affecting transcript levels by regulating ribosomal occupancy, indicating transcription-independent modulation of translation by m6A.[59] Notably, m6A has been shown to promote the localization of neuronal mRNAs to dendrites and axons or regulate local translation at axons.[60–63]

Given that m6A could affect various aspects of mRNA metabolism, we took advantage of GO clustering to explore potentially disrupted networks in MDD. However, our analysis did not fully show the direct effect of m6A in the networks. Further mechanistic investigations are essential to understand the influence of m6A on the target transcripts and how the changes contribute to the dysregulation of the networks. Future studies integrating multiomic data hold promise for providing deeper insights into these networks. Addressing these limitations in future research endeavors could offer novel insights into the molecular mechanisms underlying MDD.

RESOURCE AVAILABILITY

Lead contact

Further information and requests for resources and reagents should be made directly to and will be fulfilled by, the Lead Contact, Gustavo Turecki (gustavo.turecki@mcgill.ca).

Materials availability

This study did not generate new unique reagents.

Data and code availability

The raw sequencing data generated in this study have been deposited at GEO and are publicly available as of the date of publication. The accession number can be found in the key resources table. This study did not generate the original code. Any additional information required to reanalyze the data reported in this article is available from the lead contact upon request.

ACKNOWLEDGMENTS

GT holds a Canada Research Chair (Tier 1) and is supported by grants from the Canadian Institutes of Health Research (CIHR; FDN148374, ENP161427 [ERA-NET ERA PerMed], PJT183903, PJT189993) and National Institutes of Health (NIH; R56MH131818-01). CN holds an FRQS research scholar junior 1. We acknowledge the experts at Douglas-Bell-Canada Brain Bank. This Project has been made possible with the financial support of Health Canada, through the Canada Brain Research Fund, an innovative partnership between the Government of Canada (through Health Canada) and Brain Canada, and in part by funding from the Canada First Research Excellence Fund, awarded to McGill University for the Healthy Brains for Healthy Lives initiative, and from the Fonds de recherche du Québec - Santé (FRQS) through the Quebec Network on Suicide, Mood Disorders and Related Disorders. This research was enabled in part by support provided by Calcul Québec (https://www.calculquebec.ca/en/) and the Digital Research Alliance of Canada (alliancecan.ca). We thank Malosree Maitra for her suggestions on data interpretation. We thank Gabriella Frosi for help with data management.

AUTHOR CONTRIBUTIONS

H.M. led data curation, data analysis, data investigation, and writing. R.L. supported data investigation. A.C. supported data analysis. N.M contributed to sample procurement and article review. C.N. and G.T. supervised the study design, data investigation, and writing. C.N. and G.T. obtained funding.

DECLARATION OF INTERESTS

The authors declare no competing interests.

STAR★METHODS

Detailed methods are provided in the online version of this paper and include the following:

- KEY RESOURCES TABLE
- EXPERIMENTAL MODEL AND STUDY PARTICIPANT DETAILS
- METHOD DETAILS
  - m6A-seq
- QUANTIFICATION AND STATISTICAL ANALYSIS
  - m6a peak calling
  - Differential m6A peak analysis
  - Differential gene analysis
  - Rank-rank hypergeometric overlap (RRHO) analysis
  - Gene ontology (GO) analysis
  - Protein-protein network analysis

SUPPLEMENTAL INFORMATION

Supplemental information can be found online at https://doi.org/10.1016/j.isci.2024.111316.

Received: May 22, 2024
Revised: September 3, 2024
Accepted: October 30, 2024
Published: November 4, 2024

REFERENCES

1. Cappannini, A., Ray, A., Purta, E., Mukherjee, S., Boccaletto, P., Moafinejad, S.N., Lechner, A., Barchet, C., Klaholz, B.P., Stefaniak, F., and Bujnicki, J.M. (2024). MODOMICS: a database of RNA modifications and related information. 2023 update. Nucleic Acids Res. *52*, D239–D244. https://doi.org/10.1093/nar/gkad1083.
2. He, P.C., and He, C. (2021). m6A RNA methylation: from mechanisms to therapeutic potential. EMBO J. *40*, e105977. https://doi.org/10.15252/embj.2020105977.
3. Liu, J., Yue, Y., Han, D., Wang, X., Fu, Y., Zhang, L., Jia, G., Yu, M., Lu, Z., Deng, X., et al. (2014). A METTL3-METTL14 complex mediates mammalian nuclear RNA N6-adenosine methylation. Nat. Chem. Biol. *10*, 93–95. https://doi.org/10.1038/nchembio.1432.
4. Ping, X.L., Sun, B.F., Wang, L., Xiao, W., Yang, X., Wang, W.J., Adhikari, S., Shi, Y., Lv, Y., Chen, Y.S., et al. (2014). Mammalian WTAP is a regulatory subunit of the RNA N6-methyladenosine methyltransferase. Cell Res. *24*, 177–189. https://doi.org/10.1038/cr.2014.3.

5. Jia, G., Fu, Y., Zhao, X., Dai, Q., Zheng, G., Yang, Y., Yi, C., Lindahl, T., Pan, T., Yang, Y.G., and He, C. (2011). N6-methyladenosine in nuclear RNA is a major substrate of the obesity-associated FTO. Nat. Chem. Biol. *7*, 885–887. https://doi.org/10.1038/nchembio.687.

6. Fu, Y., Dominissini, D., Rechavi, G., and He, C. (2014). Gene expression regulation mediated through reversible m(6)A RNA methylation. Nat. Rev. Genet. *15*, 293–306. https://doi.org/10.1038/nrg3724.

7. Livneh, I., Moshitch-Moshkovitz, S., Amariglio, N., Rechavi, G., and Dominissini, D. (2020). The m6A epitranscriptome: transcriptome plasticity in brain development and function. Nat. Rev. Neurosci. *21*, 36–51. https://doi.org/10.1038/s41583-019-0244-z.

8. Mitsuhashi, H., and Nagy, C. (2023). Potential Roles of m6A and FTO in Synaptic Connectivity and Major Depressive Disorder. Int. J. Mol. Sci. *24*, 6220. https://doi.org/10.3390/ijms24076220.

9. Chang, M., Lv, H., Zhang, W., Ma, C., He, X., Zhao, S., Zhang, Z.W., Zeng, Y.X., Song, S., Niu, Y., and Tong, W.M. (2017). Region-specific RNA m(6)A methylation represents a new layer of control in the gene regulatory network in the mouse brain. Open Biol. *7*, 170166. https://doi.org/10.1098/rsob.170166.

10. Zhang, Z., Wang, M., Xie, D., Huang, Z., Zhang, L., Yang, Y., Ma, D., Li, W., Zhou, Q., Yang, Y.G., and Wang, X.J. (2018). METTL3-mediated N6-methyladenosine mRNA modification enhances long-term memory consolidation. Cell Res. *28*, 1050–1061. https://doi.org/10.1038/s41422-018-0092-9.

11. Shi, H., Zhang, X., Weng, Y.L., Lu, Z., Liu, Y., Lu, Z., Li, J., Hao, P., Zhang, Y., Zhang, F., et al. (2018). m6A facilitates hippocampus-dependent learning and memory through YTHDF1. Nature *563*, 249–253. https://doi.org/10.1038/s41586-018-0666-1.

12. Walters, B.J., Mercaldo, V., Gillon, C.J., Yip, M., Neve, R.L., Boyce, F.M., Frankland, P.W., and Josselyn, S.A. (2017). The Role of The RNA Demethylase FTO (Fat Mass and Obesity-Associated) and mRNA Methylation in Hippocampal Memory Formation. Neuropsychopharmacology *42*, 1502–1510. https://doi.org/10.1038/npp.2017.31.

13. Merkurjev, D., Hong, W.T., Iida, K., Oomoto, I., Goldie, B.J., Yamaguti, H., Ohara, T., Kawaguchi, S.Y., Hirano, T., Martin, K.C., et al. (2018). Synaptic N^6-methyladenosine (m^6A) epitranscriptome reveals functional partitioning of localized transcripts. Nat. Neurosci. *21*, 1004–1014. https://doi.org/10.1038/s41593-018-0173-6.

14. Shen, J., Yang, L., and Wei, W. (2021). Role of Fto on CaMKII/CREB signaling pathway of hippocampus in depressive-like behaviors induced by chronic restraint stress mice. Behav. Brain Res. *406*, 113227. https://doi.org/10.1016/J.BBR.2021.113227.

15. Engel, M., Eggert, C., Kaplick, P.M., Eder, M., Röh, S., Tietze, L., Namendorf, C., Arloth, J., Weber, P., Rex-Haffner, M., et al. (2018). The Role of m6A/m-RNA Methylation in Stress Response Regulation. Neuron *99*, 389–403.e9. https://doi.org/10.1016/j.neuron.2018.07.009.

16. Spencer, L., James, D.A., Abate, K.H., Abay, S.M., Abbafati, C., Abbasi, N., and Murray, C.J.L. (2018). Global, regional, and national incidence, prevalence, and years lived with disability for 354 diseases and injuries for 195 countries and territories, 1990-2017: a systematic analysis for the Global Burden of Disease Study. Lancet *392*, 1789–1858. https://doi.org/10.1016/S0140-6736(18)32279-7.

17. Nestler, E.J. (2014). Epigenetic mechanisms of depression. JAMA Psychiatr. *71*, 454–456. https://doi.org/10.1001/jamapsychiatry.2013.4291.

18. Duman, R.S., and Aghajanian, G.K. (2012). Synaptic dysfunction in depression: potential therapeutic targets. Science *338*, 68–72. https://doi.org/10.1126/science.1222939.

19. Banasr, M., Dwyer, J.M., and Duman, R.S. (2011). Cell atrophy and loss in depression: reversal by antidepressant treatment. Curr. Opin. Cell Biol. *23*, 730–737. https://doi.org/10.1016/j.ceb.2011.09.002.

20. Chedotal, A., and Richards, L.J. (2010). Wiring the brain: the biology of neuronal guidance. Cold Spring Harb Perspect Biol *2*, a001917. https://doi.org/10.1101/cshperspect.a001917.

21. Zhuang, M., Li, X., Zhu, J., Zhang, J., Niu, F., Liang, F., Chen, M., Li, D., Han, P., and Ji, S.J. (2019). The m6A reader YTHDF1 regulates axon guidance through translational control of Robo3.1 expression. Nucleic Acids Res. *47*, 4765–4777. https://doi.org/10.1093/nar/gkz157.

22. Drevets, W.C. (2000). Functional anatomical abnormalities in limbic and prefrontal cortical structures in major depression. Prog. Brain Res. *126*, 413–431. https://doi.org/10.1016/S0079-6123(00)26027-5.

23. Dominissini, D., Moshitch-Moshkovitz, S., Schwartz, S., Salmon-Divon, M., Ungar, L., Osenberg, S., Cesarkas, K., Jacob-Hirsch, J., Amariglio, N., Kupiec, M., et al. (2012). Topology of the human and mouse m6A RNA methylomes revealed by m6A-seq. Nature *485*, 201–206. https://doi.org/10.1038/nature11112.

24. Xiong, X., Hou, L., Park, Y.P., Molinie, B., GTEx Consortium; Kellis, M., Gregory, R.I., Gregory, R.I., and Kellis, M. (2021). Genetic drivers of m6A methylation in human brain, lung, heart and muscle. Nat. Genet. *53*, 1156–1165. https://doi.org/10.1038/s41588-021-00890-3.

25. Castro-Hernández, R., Berulava, T., Metelova, M., Epple, R., Centeno, T.P., Sakib, S., Burkhart, S., Ninov, M., Bohnsack, K.E., Bohnsack, M.T., et al. (2022). Conserved reduction of m6A marks during aging and neurodegeneration is linked to altered translation of synaptic transcripts. Preprint at bioRxiv. https://doi.org/10.1101/2022.06.08.495100.

26. Labonte, B., Engmann, O., Purushothaman, I., Menard, C., Wang, J., Tan, C., Scarpa, J.R., Moy, G., Loh, Y.E., Cahill, M., et al. (2017). Sex-specific transcriptional signatures in human depression. Nat Med *23*, 1102–1111. https://doi.org/10.1038/nm.4386.

27. Seney, M.L., Huo, Z., Cahill, K., French, L., Puralewski, R., Zhang, J., Logan, R.W., Tseng, G., Lewis, D.A., and Sibille, E. (2018). Opposite molecular signatures of depression in men and women. Biol. Psychiatry *84*, 18–27. https://doi.org/10.1016/j.biopsych.2018.01.017.

28. Maitra, M., Mitsuhashi, H., Rahimian, R., Chawla, A., Yang, J., Fiori, L.M., Davoli, M.A., Perlman, K., Aouabed, Z., Mash, D.C., et al. (2023). Cell type specific transcriptomic differences in depression show similar patterns between males and females but implicate distinct cell types and genes. Nat. Commun. *14*, 2912. https://doi.org/10.1038/s41467-023-38530-5.

29. Mansouri, S., Pessoni, A.M., Marroquín-Rivera, A., Parise, E.M., Tamminga, C.A., Turecki, G., Nestler, E.J., Chen, T.H., and Labonté, B. (2023). Transcriptional dissection of symptomatic profiles across the brain of men and women with depression. Nat. Commun. *14*, 6835. https://doi.org/10.1038/s41467-023-42686-5.

30. Reis, A.L.M., Hammond, J.M., Stevanovski, I., Arnold, J.C., McGregor, I.S., Deveson, I.W., and Gururajan, A. (2022). Sex-specific transcriptomic and epitranscriptomic signatures of PTSD-like fear acquisition. iScience *25*, 104861. https://doi.org/10.1016/J.ISCI.2022.104861.

31. Torres-Berrio, A., Hernandez, G., Nestler, E.J., and Flores, C. (2020). The Netrin-1/DCC Guidance Cue Pathway as a Molecular Target in Depression: Translational Evidence. Biol Psychiatry *88*, 611–624. https://doi.org/10.1016/j.biopsych.2020.04.025.

32. Matsunaga, E., Nakamura, H., and Chédotal, A. (2006). Repulsive guidance molecule plays multiple roles in neuronal differentiation and axon guidance. J. Neurosci. *26*, 6082–6088. https://doi.org/10.1523/JNEUROSCI.4556-05.2006.

33. Liu, S., Xiu, J., Zhu, C., Meng, K., Li, C., Han, R., Du, T., Li, L., Xu, L., Liu, R., et al. (2021). Fat mass and obesity-associated protein regulates RNA methylation associated with depression-like behavior in mice. Nat. Commun. *12*, 6937. https://doi.org/10.1038/s41467-021-27044-7.

34. Joshi, K., Wang, D.O., and Gururajan, A. (2022). The m6A-methylome in major depression: A bioinformatic analysis of publicly available datasets. Psychiatry Res. Commun. *2*, 100089. https://doi.org/10.1016/j.psycom.2022.100089.

35. Osmanbeyoglu, H.U., Lu, K.N., Oesterreich, S., Day, R.S., Benos, P.V., Coronnello, C., and Lu, X. (2013). Estrogen represses gene expression through reconfiguring chromatin structures. Nucleic Acids Res. *41*, 8061–8071. https://doi.org/10.1093/nar/gkt586.

36. Kovacs, T., Szabo-Meleg, E., and Abraham, I.M. (2020). Estradiol-Induced Epigenetically Mediated Mechanisms and Regulation of Gene Expression. Int. J. Mol. Sci. *21*, 3177. https://doi.org/10.3390/ijms21093177.

37. Stevens, T.A., and Meech, R. (2006). BARX2 and estrogen receptor-alpha (ESR1) coordinately regulate the production of alternatively spliced ESR1 isoforms and control breast cancer cell growth and invasion. Oncogene *25*, 5426–5435. https://doi.org/10.1038/sj.onc.1209529.

38. Wan, S., Sun, Y., Zong, J., Meng, W., Yan, J., Chen, K., Wang, S., Guo, D., Xiao, Z., Zhou, Q., et al. (2023). METTL3-dependent m6A methylation facilitates uterine receptivity and female fertility via balancing estrogen and progesterone signaling. Cell Death Dis. *14*, 6–14. https://doi.org/10.1038/s41419-023-05866-1.

39. Kan, R.L., Chen, J., and Sallam, T. (2022). Crosstalk between epitranscriptomic and epigenetic mechanisms in gene regulation. Trends Genet. *38*, 182–193. https://doi.org/10.1016/j.tig.2021.06.014.

40. Maldonado Lopez, A.M., Ko, E.K., Huang, S., Pacella, G., Kuprasertkul, N., D'Souza, C.,A., Reyes Hueros, R.A., Shen, H., Stoute, J., Elashal, H., et al. (2023). Mettl3-catalyzed m6A regulates histone modifier and modification expression in self-renewing somatic tissue. Sci. Adv. *9*, 35. https://doi.org/10.1126/sciadv.adg5234.

41. Papale, L.A., Li, S., Madrid, A., Zhang, Q., Chen, L., Chopra, P., Jin, P., Keleş, S., and Alisch, R.S. (2016). Sex-specific hippocampal 5-hydroxymethylcytosine is disrupted in response to acute stress. Neurobiol. Dis. *96*, 54–66.

42. Covington, H.E., 3rd, Maze, I., LaPlant, Q.C., Vialou, V.F., Ohnishi, Y.N., Berton, O., Fass, D.M., Renthal, W., Rush, A.J., 3rd, Wu, E.Y., et al. (2009). Antidepressant actions of histone deacetylase inhibitors. J. Neurosci. *29*, 11451–11460. https://doi.org/10.1523/JNEUROSCI.1758-09.2009.

43. Alhassen, W., Chen, S., Vawter, M., Robbins, B.K., Nguyen, H., Myint, T.N., Saito, Y., Schulmann, A., Nauli, S.M., Civelli, O., et al. (2021). Patterns of cilia gene dysregulations in major psychiatric disorders. Prog. Neuro-Psychopharmacol. Biol. Psychiatry *109*, 110255. https://doi.org/10.1016/j.pnpbp.2021.110255.

44. Sterpka, A., and Chen, X. (2018). Neuronal and Astrocytic Primary Cilia in the Mature Brain. Pharmacol. Res. *137*, 114–121.

45. Wachten, D., and Mick, D.U. (2021). Signal transduction in primary cilia - analyzing and manipulating GPCR and second messenger signaling. Pharmacol. Ther. *224*, 107836. https://doi.org/10.1016/j.pharmthera.2021.107836.

46. Catapano, L.A., and Manji, H.K. (2007). G protein-coupled receptors in major psychiatric disorders. Biochim. Biophys. Acta *1768*, 976–993. https://doi.org/10.1016/j.bbamem.2006.09.025.

47. Mantas, I., Saarinen, M., Xu, Z.Q.D., and Svenningsson, P. (2022). Update on GPCR-based targets for the development of novel antidepressants. Mol. Psychiatry *27*, 534–558. https://doi.org/10.1038/s41380-021-01040-1.

48. Seney, M.L., Glausier, J., and Sibille, E. (2022). Large-Scale Transcriptomics Studies Provide Insight Into Sex Differences in Depression. Biol. Psychiatry *91*, 14–24. https://doi.org/10.1016/j.biopsych.2020.12.025.

49. Bollinger, J.L. (2021). Uncovering microglial pathways driving sex-specific neurobiological effects in stress and depression. Brain Behav. Immun. Health *16*, 100320. https://doi.org/10.1016/j.bbih.2021.100320.

50. Isaksen, T.J., Fujita, Y., and Yamashita, T. (2020). Repulsive Guidance Molecule A Suppresses Adult Neurogenesis. Stem Cell Rep. *14*, 677–691. https://doi.org/10.1016/j.stemcr.2020.03.003.

51. Horn, K.E., Glasgow, S.D., Gobert, D., Bull, S.J., Luk, T., Girgis, J., Tremblay, M.E., McEachern, D., Bouchard, J.F., Haber, M., et al. (2013). DCC expression by neurons regulates synaptic plasticity in the adult brain. Cell Rep. *3*, 173–185. https://doi.org/10.1016/j.celrep.2012.12.005.

52. Glasgow, S.D., Labrecque, S., Beamish, I.V., Aufmkolk, S., Gibon, J., Han, D., Harris, S.N., Dufresne, P., Wiseman, P.W., McKinney, R.A., et al. (2018). Activity-Dependent Netrin-1 Secretion Drives Synaptic Insertion of GluA1-Containing AMPA Receptors in the Hippocampus. Cell Rep. *25*, 168–182.e6. https://doi.org/10.1016/j.celrep.2018.09.028.

53. Torres-Berrio, A., Lopez, J.P., Bagot, R.C., Nouel, D., Dal Bo, G., Cuesta, S., Zhu, L., Manitt, C., Eng, C., Cooper, H.M., et al. (2017). DCC Confers Susceptibility to Depression-like Behaviors in Humans and Mice and Is Regulated by miR-218. Biol Psychiatry *81*, 306–315. https://doi.org/10.1016/j.biopsych.2016.08.017.

54. Diab, A.M., Wigerius, M., Quinn, D.P., Qi, J., Shahin, I., Paffile, J., Krueger, K., Karten, B., Krueger, S.R., and Fawcett, J.P. (2023). NCK1 Modulates Neuronal Actin Dynamics and Promotes Dendritic Spine, Synapse, and Memory Formation. J. Neurosci. *43*, 885–901.

55. Meyer, K.D. (2019). DART-seq: an antibody-free method for global m6A detection. Nat. Methods *16*, 1275–1280. https://doi.org/10.1038/s41592-019-0570-0.

56. Tegowski, M., Flamand, M.N., and Meyer, K.D. (2022). scDART-seq reveals distinct m6A signatures and mRNA methylation heterogeneity in single cells. Mol. Cell *82*, 868–878.e10. https://doi.org/10.1016/J.MOLCEL.2021.12.038.

57. Hendra, C., Pratanwanich, P.N., Wan, Y.K., Goh, W.S.S., Thiery, A., and Göke, J. (2022). Detection of m6A from direct RNA sequencing using a multiple instance learning framework. Nat. Methods *19*, 1590–1598. https://doi.org/10.1038/s41592-022-01666-1.

58. Nagy, C., Maitra, M., Tanti, A., Suderman, M., Théroux, J.F., Davoli, M.A., Perlman, K., Yerko, V., Wang, Y.C., Tripathy, S.J., et al. (2020). Single-nucleus transcriptomics of the prefrontal cortex in major depressive disorder implicates oligodendrocyte precursor cells and excitatory neurons. Nat. Neurosci. *23*, 771–781. https://doi.org/10.1038/s41593-020-0621-y.

59. Berulava, T., Buchholz, E., Elerdashvili, V., Pena, T., Islam, M.R., Lbik, D., Mohamed, B.A., Renner, A., von Lewinski, D., Sacherer, M., et al. (2020). Changes in m6A RNA methylation contribute to heart failure progression by modulating translation. Eur. J. Heart Fail. *22*, 54–66. https://doi.org/10.1002/EJHF.1672.

60. Martinez De La Cruz, B., Markus, R., Malla, S., Haig, M.I., Gell, C., Sang, F., Bellows, E., Sherif, M.A., McLean, D., Lourdusamy, A., et al. (2021). Modifying the m6A brain methylome by ALKBH5-mediated demethylation: a new contender for synaptic tagging. Mol. Psychiatry *26*, 7141–7153. https://doi.org/10.1038/s41380-021-01282-z.

61. Flamand, M.N., and Meyer, K.D. (2022). m6A and YTHDF proteins contribute to the localization of select neuronal mRNAs. Nucleic Acids Res. *50*, 4464–4483. https://doi.org/10.1093/NAR/GKAC251.

62. Yu, J., Chen, M., Huang, H., Zhu, J., Song, H., Zhu, J., Park, J., and Ji, S.J. (2018). Dynamic m6A modification regulates local translation of mRNA in axons. Nucleic Acids Res. *46*, 1412–1423. https://doi.org/10.1093/NAR/GKX1182.

63. Madugalle, S.U., Meyer, K., Wang, D.O., and Bredy, T.W. (2020). RNA N 6-Methyladenosine and the Regulation of RNA Localization and Function in the Brain. Trends Neurosci. *43*, 1011–1023. https://doi.org/10.1016/J.TINS.2020.09.005.

64. Labuda, M., Labuda, D., Korab-Laskowska, M., Cole, D.E., Zietkiewicz, E., Weissenbach, J., Popowska, E., Pronicka, E., Root, A.W., and Glorieux, F.H. (1996). Linkage disequilibrium analysis in young populations: pseudo-vitamin D-deficiency rickets and the founder effect in French Canadians. Am. J. Hum. Genet. *59*, 633–643.

65. Marcel, M. (2011). Cutadapt Removes Adapter Sequences From High-Throughput Sequencing Reads. EMBnet J. *17*, 10. https://doi.org/10.14806/ej.17.1.200.

66. Dobin, A., Davis, C.A., Schlesinger, F., Drenkow, J., Zaleski, C., Jha, S., Batut, P., Chaisson, M., and Gingeras, T.R. (2013). STAR: ultrafast universal RNA-seq aligner. Bioinformatics *29*, 15–21. https://doi.org/10.1093/bioinformatics/bts635.

67. Kopylova, E., Noé, L., and Touzet, H. (2012). SortMeRNA: fast and accurate filtering of ribosomal RNAs in metatranscriptomic data. Bioinformatics *28*, 3211–3217. https://doi.org/10.1093/bioinformatics/bts611.

68. Yu, G., Wang, L.G., and He, Q.Y. (2015). ChIPseeker: an R/Bioconductor package for ChIP peak annotation, comparison and visualization. Bioinformatics *31*, 2382–2383. https://doi.org/10.1093/bioinformatics/btv145.

69. Bailey, T.L., Johnson, J., Grant, C.E., and Noble, W.S. (2015). The MEME Suite. Nucleic Acids Res. *43*, W39–W49. https://doi.org/10.1093/nar/gkv416.

70. Cui, X., Wei, Z., Zhang, L., Liu, H., Sun, L., Zhang, S.W., Huang, Y., and Meng, J. (2016). Guitar: An R/Bioconductor Package for Gene Annotation Guided Transcriptomic Analysis of RNA-Related Genomic Features. BioMed Res. Int. *2016*, 8367534. https://doi.org/10.1155/2016/8367534.

71. Guo, Z., Shafik, A.M., Jin, P., and Wu, H. (2022). Differential RNA methylation analysis for MeRIP-seq data under general experimental design. Bioinformatics *38*, 4705–4712. https://doi.org/10.1093/bioinformatics/btac601.

72. Liao, Y., Smyth, G.K., and Shi, W. (2013). The Subread aligner: fast, accurate and scalable read mapping by seed-and-vote. Nucleic Acids Res. *41*, e108. https://doi.org/10.1093/nar/gkt214.

73. Love, M.I., Huber, W., and Anders, S. (2014). Moderated estimation of fold change and dispersion for RNA-seq data with DESeq2. Genome Biol. *15*, 550. https://doi.org/10.1186/s13059-014-0550-8.

74. Cahill, K.M., Huo, Z., Tseng, G.C., Logan, R.W., Seney, M.L., Cahill, K.M., Huo, Z., Tseng, G.C., Logan, R.W., and Seney, M.L. (2018). Improved identification of concordant and discordant gene expression signatures using an updated rank-rank hypergeometric overlap approach. Sci. Rep. *8*, 9588. https://doi.org/10.1038/s41598-018-27903-2.

75. Yu, G., Wang, L.G., Han, Y., and He, Q.Y. (2012). clusterProfiler: an R package for comparing biological themes among gene clusters. OMICS *16*, 284–287. https://doi.org/10.1089/omi.2011.0118.

76. Brionne, A., Juanchich, A., and Hennequet-Antier, C. (2019). ViSEAGO: a Bioconductor package for clustering biological functions using Gene Ontology and semantic similarity. BioData Min. *12*, 16. https://doi.org/10.1186/s13040-019-0204-1.

77. Szklarczyk, D., Gable, A.L., Lyon, D., Junge, A., Wyder, S., Huerta-Cepas, J., Simonovic, M., Doncheva, N.T., Morris, J.H., Bork, P., et al. (2019). STRING v11: protein-protein association networks with increased coverage, supporting functional discovery in genome-wide experimental datasets. Nucleic Acids Res. *47*, D607–D613. https://doi.org/10.1093/nar/gky1131.

78. Shannon, P., Markiel, A., Ozier, O., Baliga, N.S., Wang, J.T., Ramage, D., Amin, N., Schwikowski, B., and Ideker, T. (2003). Cytoscape: a software environment for integrated models of biomolecular interaction networks. Genome Res. *13*, 2498–2504. https://doi.org/10.1101/gr.1239303.

STAR★METHODS

KEY RESOURCES TABLE

REAGENT or RESOURCE	SOURCE	IDENTIFIER
Antibodies		
m6A antibody	Synaptic Systems	Cat#202003
Biological samples		
Postmortem human brain (ventromedial prefrontal cortex)	Douglas-Bell-Canada Brain Bank	N/A
Chemicals, peptides, and recombinant proteins		
protein-A magnetic beads	Thermo Fisher Scientific	Cat#10001D
protein-A magnetic beads	Thermo Fisher Scientific	Cat#10003D
RNA inhibitor	Promega	Cat#2611
Critical commercial assays		
RNeasy Lipid Tissue Mini Kit	QIAGEN	Cat#74804
RNA Clean and Concentrator	Zymo Research	Cat#R1015
SMARTer Stranded Total RNA-Seq Kit v2	Takara	Cat#634412
Deposited data		
Sequencing data	This paper	GEO: GSE275676
Software and algorithms		
Rstudio	https://www.rstudio.com/products/rstudio	Version 1.2.5033
GraphPad Prism	https://www.graphpad.com/	Version 9
STRING	https://string-db.org/	Version 12.0
Cytoscape	https://cytoscape.org/	Version 3.10.1

EXPERIMENTAL MODEL AND STUDY PARTICIPANT DETAILS

Human postmortem tissue from ventromedial prefrontal cortex (vmPFC) was obtained from the Douglas-Bell-Canada Brain Bank (douglasbrainbank.ca), in collaboration with the Quebec Coroner's Office. All individuals were French-Canadian origin, a homogeneous population with a well-documented founder effect.[64] Comprehensive psychological autopsies were conducted. Briefly, these consist of a series of proxy-based, structured interviews assessing psychopathology with next-of-kin and reviews of medical records. Cases were individuals who died by suicide in the context of an episode of MDD. Controls were individuals who died suddenly and did not have evidence of an axis I disorder. Groups were matched for postmortem interval (PMI), tissue pH, and RNA Integrity number (Table S1). This project was approved by the Douglas Hospital Research Center institutional Ethic review board.

METHOD DETAILS

m6A-seq

Total RNA was extracted from postmortem brain tissues using RNeasy Lipid Tissue Mini Kit (QIAGEN, #74804) following the manufacturer's instructions. RNA was treated with DNase during this process. Total RNA was then fragmented to ~200nt using focused-ultrasonicator (Covaris, #S220). A portion of the RNA was reserved as inputs, while remaining was subjected into immunoprecipitation. First, 30ul of protein-A magnetic beads (Thermo Fisher Scientific, #10001D) and 30ul of protein-G magnetic beads (Thermo Fisher Scientific, #10003D) were washed twice with 500ul of IP buffer (10mM Tris-HCl (pH 7.4), 150mM NaCl, and 0.1% (v/v) Igepal CA-630). The beads were resuspended with a mixture of 500ul of IP buffer and 1ug of an anti-m6A antibody (Synaptic Systems, #202003) and incubated at 4°C overnight. The resulting antibody-bead complexes were washed 2 times with 500uL of IP buffer. The antibody-bead complexes were then mixed with 500uL of IP mixture composed of 20ug of the RNA, 100uL of 5X IP buffer, and 5uL of RNA inhibitor (Promega, #2611). After incubating at 4°C for 2 h, the mixture was washed intensively: twice by 500uL of IP buffer, twice by 500uL of low salt buffer (10mM Tris-HCl (pH 7.4), 50mM NaCl, and 0.1% (v/v) Igepal CA-630), and twice by 500uL of high salt IP buffer (10mM Tris-HCl (pH 7.4), 500mM NaCl, and 0.1% (v/v) Igepal CA-630). The RNA was eluted with 100uL of RLT buffer and purified using RNA Clean and Concentrator (Zymo Research, #R1015). The average total IP yield of 8.7ng was obtained. The purified IP-RNA and input-RNA were subjected into SMARTer Stranded Total RNA-Seq Kit v2 (Takara, #634412),

and cDNA libraries were generated following the manufacturer's instructions. The libraries were sequenced at the McGill University and Genome Quebec Innovation Center (Montreal, Canada) on an Illumina NovaSeq 6000 platform with 100nt paired-end mode.

QUANTIFICATION AND STATISTICAL ANALYSIS

m6a peak calling

Adapters were trimmed using TrimGalore.[65] The trimmed reads were aligned to GRCh38 human genome using STAR.[66] rRNA contamination was removed from all the alignments on the basis rRNA co-ordinates bed file of the GRCh38 genome using SortMeRNA.[67] m6a peaks in individual sample for consensus m6A peaks were identified using TRESS using the default parameters with lowcount = 15. The peaks with false discovery rate (FDR) < 0.05 and fold change >1.5 were applied to extract confidential peaks and used for downstream analysis. The peaks were annotated using ChiPseeker.[68] Motif enrichment analysis was conducted using findMotifsGenme.pl function from homer. For each sample, the enrichment of the m6A consensus motif GGACH was calculated using AME from MEME tools and accumulative proportion was calculated.[69] The distribution of m6A peaks on mRNA was visualized using Guitar.[70]

Differential m6A peak analysis

Differential methylation region (DMR) analysis was carried out using TRESS.[71] TRESS uses a hierarchical negative binomial model to account for sources of variation and implements a linear model to design complex contrasts of interest. A wald test is used for hypothesis testing and to identify DMR. Parameters with Binsize = 50 and lowcount = 15 were used. In addition, based on the level of correlation between the PC variances and known variables, RIN and age were included as covariates for all the DMR analysis. Significant DMRs were identified using a threshold of nominal p-value <0.05 and fold change >1.2.

Differential gene analysis

Gene counts for the GRCh38 genome was obtained using Subread[72] after removing rRNA contamination. Gene with low counts, supported by less than 50% of the samples, were removed prior to the analysis. Differential gene (DEG) analysis was conducted using DESeq2 which uses negative binomial generalized linear model with a default parameter.[73] Similar to m6A-seq analysis, age and RIN were included as covariates. Threshold of a nominal p-value <0.05 and fold change >1.2 were used for DEG criteria and used for downstream analysis.

Rank-rank hypergeometric overlap (RRHO) analysis

RRHO analysis was to compare the overall methylation patterns between male MDD and female MDD using RRHO2.[74] In this analysis, the entire gene list from each dataset is ranked based on the methylation score calculated as -log10(p-value)*sign(logFoldChange). These ranks are then arranged vertically or horizontally to visualize the overlap intensity between the datasets. RRHO algorithm calculates the significance values for each overlapping gene pair, representing the degree of overlap between the datasets, and constructs a significance matrix. This matrix is then visualized as a heatmap, where each point represents the significance of the overlap according to the hypergeometric distribution.

Gene ontology (GO) analysis

GO analysis for biological processes was conducted using the clusterProfiler,[75] employing a cutoff of p-value <0.05. The top 5 GO terms for each category, based on their nominal p-values, were visualized. To compare shared GO terms between DMR and DEG datasets, the ViSEAGO[76] was used for GO clustering across the two experiments. ViSEAGO first computes semantic similarity between pairs of GO terms to capture likeness between biological features represented by GO terms. After calculating the distance between sets of GO terms, hierarchical clustering based on semantic similarity using Ward's method is performed. Among the GO clusters, a key GO cluster was selected by first filtering GO term by -log10(p-value) > 1.0 in both DMR and DEG datasets. Then GO terms were ordered according to p-values in DMR sets. GO clusters with the lowest p-values in the DMR dataset was selected for further investigation.

Protein-protein network analysis

The PPI analysis was conducted using STRING[77] to evaluate interactions among the protein products of DMR-genes and DEGs. The list of DMR-genes and DEGs assigned to the GO cluster was provided as input and filtered for an interaction score greater than 0.4. Additionally, proteins with no interactions with other proteins were excluded from the analysis. The resulting network was visualized using Cytoscape,[78] with node size corresponding to the degree of interaction, node color indicating the differential expression status, node edge color signifying differential methylation, and edge width reflecting the interaction score.